



Enhancement of the fatigue strength by application of a low transformation temperature (LTT) welding consumable

Martin Huebner¹ · Florian Dittmann² · Arne Kromm¹ · Igor Varfolomeev² · Thomas Kannengiesser¹

Received: 6 November 2025 / Accepted: 16 January 2026
© The Author(s) 2026

Abstract

Low transformation temperature (LTT) welding consumables offer the possibility of enhancing fatigue strength in welded components without post-treatment. By lowering the martensite start temperature (M_S), the volume expansion during transformation near ambient temperature is reduced, which decreases welding-related tensile residual stresses in fatigue-critical areas. To evaluate this effect, longitudinal stiffeners were used. To evaluate this effect, longitudinal stiffeners were used, a LTT and conventional filler serve as welding consumable; also, high frequency mechanical impact (HFMI) treatment was carried out. Three single-pass and six additional-pass sample series were investigated for residual stress and fatigue strength. The additional welds were applied in fatigue-cracked critical areas with different weld shapes, achieved by varying welding parameters. Mechanical tests on reference samples evaluated the properties of the diluted LTT welds. Although reduced toughness was observed, no fatigue cracks occurred in LTT single-pass weld roots. The fatigue strength at two million cycles increased from 81 to 121 MPa compared to conventional welds, while HFMI reached 146 MPa. With an additional LTT weld pass, the results varied from 138 to 196 MPa, depending on the shape and residual stress state. The results show that LTT fillers effectively enhance fatigue performance, and that weld geometry and parameter selection are as critical as the chemical composition for maximizing the LTT effect.

Keywords Low transformation temperature welding consumables (LTT) · Martensite start temperature · Residual stress · Fatigue strength · Longitudinal stiffener

1 Introduction/state of the art

Increasing fatigue strength is essential for welded steel constructions that are subject to cyclic loads. Beside design conditions such as a smart welding sequence or the weld geometry improvement, residual stresses often have a crucial impact on fatigue strength. Those stresses often make structures sensitive to cyclic loads, as they reach their highest concentrations in fatigue critical areas [1–4]. To increase the fatigue strength, there are several post-treatment processes

which reduce tensile residual stresses and/or geometric notches and/or cause local work hardening. These processes include TIG-Dressing, grinding, clean blasting, and high-frequency mechanical impact treatment (HFMI). HFMI, in particular, is currently the subject of investigations in various studies. This is because high compressive residual stresses are induced, the geometric notch at the weld toe is considerably reduced, and work-hardening effects occur in the fatigue crack zone [5–8].

The previously mentioned techniques require an additional process step after welding, which causes additional costs and time. An alternative approach is to introduce compressive residual stress during the welding process and cooling, respectively. This can be achieved by using the volume expansion in the weld filler metal during the austenite → martensite transformation, which reduces tensile residual stress and partly generates compressive residual stress in weld metal and the surrounding heat-affected zone (HAZ). The maximum effect is obtained when the martensite start temperature (M_S) takes place close to room temperature.

Recommended for publication by Commission II - Arc Welding and Filler Metals

✉ Martin Huebner
martin.huebner@bam.de

¹ Bundesanstalt Für Materialforschung Und -Prüfung (BAM),
Unter Den Eichen 87, 12205 Berlin, Germany

² Fraunhofer Institut Für Werkstoffmechanik IWM,
Wöhlerstraße 11, 79108 Freiburg, Germany

These welding consumables are therefore referred to as low transformation temperature (LTT) welding fillers, the reduction of tensile residual stress is called “LTT-effect”. The reduction in M_S is achieved by adding chromium and nickel, which lead to an expansion of the austenite zone and thus a reduction in M_S . Previous research has demonstrated a reduction in tensile residual stress due to the LTT-effect [9–11]. To quantify the LTT-effect more precisely, Dilatometer tests were carried out, and in addition to M_S , the relative length change between M_S and room temperature was also determined, the so-called final expansion strain (FES). The greater this difference, the greater the LTT-effect [12–14]. The dilution of the LTT welding consumable with the base material is also a factor for the LTT effect. Usually, the dilution leads to an increase in M_S , as the M_S decreasing elements nickel and chromium are reduced in the solid LTT weld [13, 15].

Fatigue strength tests with LTT welding consumables have been conducted over the past two decades. Many of these studies have shown an increase in fatigue strength compared to conventional welding consumables [16–18]. A statistical analysis by Bartsch [19] found an overall improvement when using LTT filler in butt welds and longitudinal stiffeners. Longitudinal stiffeners are often used as test specimens in fatigue tests. The stiffener, which is welded to the base plate, prevents distortion of the base plate, which results in high tensile residual stresses at the weld toe of the face ends. Consequently, a longer stiffener results in a lower fatigue rating class, e.g., Eurocode 3 or the IIW recommendations [20, 21]. This in turn means that treatments to reduce residual stress can have a particularly positive effect on increasing service life. These specimen shapes are close to practical application, as stiffeners are often essential in thinner steel structures to prevent buckling or kinking.

Depending on the chemical composition, in some cases LTT alloys exhibit a reduced toughness compared to conventional welds [22, 23]. The reduced toughness was presumably responsible for fatigue cracks in the weld root in butt welds (with gaps) [22], which resulted in a significantly lower rating in IIW design recommendations [21], as crack initiation and propagation are not detectable visually. To overcome this problem, Shiga et al. [24] and Hensel et al. [22] used a combination of conventional and LTT welding consumables on longitudinal stiffeners. The root pass was welded with conventional filler (high toughness, lower fatigue strength), and an additional LTT pass was added on the fatigue-critical end faces. Both studies exhibited a significant improvement in fatigue strength when using LTT welding consumables in longitudinal stiffeners. The fatigue results were without root cracks in the study by Hensel et al. [22]; however, the results were with root cracks in the study by Shiga et al. [24], which suggests that the

high fatigue resistance of the additional LTT pass shifted the crack initiation into the root. In a previous paper, this combined approach was applied to longitudinal stiffeners where the welding parameters (speed, offset, and wire feed) were varied for one additional LTT weld bead. Despite varying geometric results, the dilution of the LTT weld remained nearly similar, and therefore, the M_S and the FES. Nevertheless, there were differences in the residual stress, which were explained by the different weld geometries [15]. The approach of the additional weld layer at the front face appears promising; however, there are still some questions that have been answered only in limited detail in the literature, which are:

1. Does an additional LTT weld pass, compared with a one-weld pass, have a significant influence on fatigue strength, and can this be influenced by varying the welding parameters?
2. A root crack propagation appears in longitudinal stiffeners when using LTT as a single pass?

To clarify these questions, this paper focuses on comparing the fatigue strength between one-pass and double-pass welded longitudinal stiffeners. The second LTT pass is varied, similar to the previously mentioned investigation [15], to generate different weld geometries.

2 Materials and methods

2.1 Materials

As base Material served a thermomechanical rolled structural steel of grade S700M and a thickness of 8 mm. As conventional filler metal a commercially available G69 solid wire electrode [25] with a diameter of 1.2 mm was used, which is matching to the steel grade S700M. The LTT filler metal is a non-commercial metal cored wire (diameter 1.2 mm) alloyed with 12 wt% chromium and 5 wt% nickel. This electrode has been successfully used in previous LTT research projects [15, 22]. The chemical composition of the undiluted materials is given in Table 1. While the base material and LTT filler were measured by optical emission spectroscopy, the composition of the conventional filler was given by the data sheet. In Table 2, the mechanical properties of the undiluted materials are listed. The calculation of M_S was carried out using Eq. (1) from Steven and Haynes [26], which had also been proven useful in previous research projects [15, 27]. Equation (1), the martensite start temperature calculation from Steven and Haynes [26], is calculated as follows:

$$M_S(^{\circ}C) = 561 - C * 474 - Mn * 33 - Cr * 17 - Ni * 17 - Mo * 21 \quad (1)$$

Table 1 Chemical composition of the undiluted material (weight percent)

| Material | C | Si | Mn | Cr | Ni | Mo | Al | Nb | V | Ti | Fe |
|---------------|-------|-------|------|-------|-------|-------|------|------|-------|------|-----|
| Base material | 0.064 | > 0.1 | 2.0 | > 0.1 | > 0.1 | > 0.1 | 0.06 | 0.04 | > 0.1 | 0.16 | Bal |
| Conv. filler | 0.09 | 0.5 | 1.57 | 0.3 | 1.4 | 0.25 | - | - | 0.09 | - | Bal |
| LTT filler | 0.04 | 0.41 | 0.75 | 11.66 | 4.73 | 0.03 | - | - | - | - | Bal |

Table 2 Mechanical properties and the calculated martensite start temperature of the undiluted materials

| Material | σ_y (MPa) | σ_{US} (MPa) | A_G (%) | Impact toughness at 20 °C (J) | M_S (°C) |
|------------------------|------------------|---------------------|-----------|-------------------------------|------------|
| Base material | ≥ 700 | ≥ 770 | ≥ 10 | ≥ 40 | - |
| Conv. filler | ≥ 690 | ≥ 790 | ≥ 16 | ≥ 47 | 412 |
| LTT filler [22] | 994 | 1121 | 11.3 | 21 | 238 |

2.2 Welding setup

This study was carried out on welded longitudinal stiffeners. The stiffener was welded to the frame on one side with a single weld pass. An additional weld pass was partially welded on the end faces. The dimensions are given in Fig. 1. The metal sheets were cut by saw (base plate) and water jet cutting (stiffener) and sand clean blasted at a pressure of 7 bar. The base plate and stiffening plate were tacked in the middle of the stiffener before welding. The welding process was gas metal arc welding (GMAW) using direct current and metal active gas (MAG). The samples were manufactured on a 5-axis welding portal with an automatic control unit, which ensured reproducible quality of the joints. The first weld pass was welded in one complete layer with conventional or LTT weld filler, with the start and end points located in the middle of the stiffening plate. The welding parameters for the first weld pass are listed in Table 3. An additional ten specimens with a conventional weld pass were HFMI treated. The procedure was pneumatic impact treatment (PIT). A hardened steel pin impacts the weld toe at a high rate, causing plastic deformation on the surface. This process introduces tensile residual stress while also hardening the near-surface layer [28]. The execution was carried out manually on the entire weld toe of the base plate. The parameters for HFMI treatment are: a frequency of 90 Hz, a

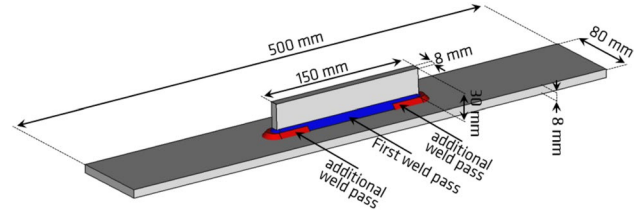


Fig. 1 Schematic shape and dimensions of the used longitudinal stiffener with the first and additional weld passes

pressure of 6 bar, a pin radius of 2 mm, and a travel speed of approximately $V_f = 20$ cm/min, which is in the recommended range of $V_f = 12$ mm/s to $V_f = 24$ mm/s for HFMI treatment after Marquis et al. [29].

The additional weld pass at the end faces of the stiffener was welded using LTT and a conventional filler material. Five different LTT shapes were generated by changing the welding parameters, which are offset from the first layer, the welding speed, the wire feed speed, and the welding torch angle. The different welding parameters are listed in Table 4. For reasons of comparison, variant 1 (offset $\uparrow\uparrow$) was also performed with a conventional welding filler as the second weld bead. For all samples with an additional pass, the conventional filler was always used for the first layer in order to ensure sufficient toughness in the weld root. This gives a test matrix with a total of nine sample series, which is summarized in Fig. 2.

2.3 Materials characterization

The material properties were characterized using macro samples. The samples were taken longitudinally from a V-butt weld with two weld passes to achieve a similar dilution of the weld as in the fatigue tested stiffeners, illustrated in Fig. 3. Two plates were welded, one with conventional weld metal and one with LTT weld metal. S700 served as

Table 3 Welding parameters for the first weld pass

| Process | Voltage | Current | Welding speed straight | Shielding gas |
|-------------------|-------------------------|------------------|-------------------------------|----------------------------|
| GMAW/MAG | 30–32 V | 240–245 A | 60 cm/min | M21 (18% CO ₂) |
| Arc energy | Welding position | Wire feed | Welding speed rotation | Preheating |
| 0.72–0.78 kJ/mm | 2F or PB (45°) | 9 m/min | 60 cm/min | none |

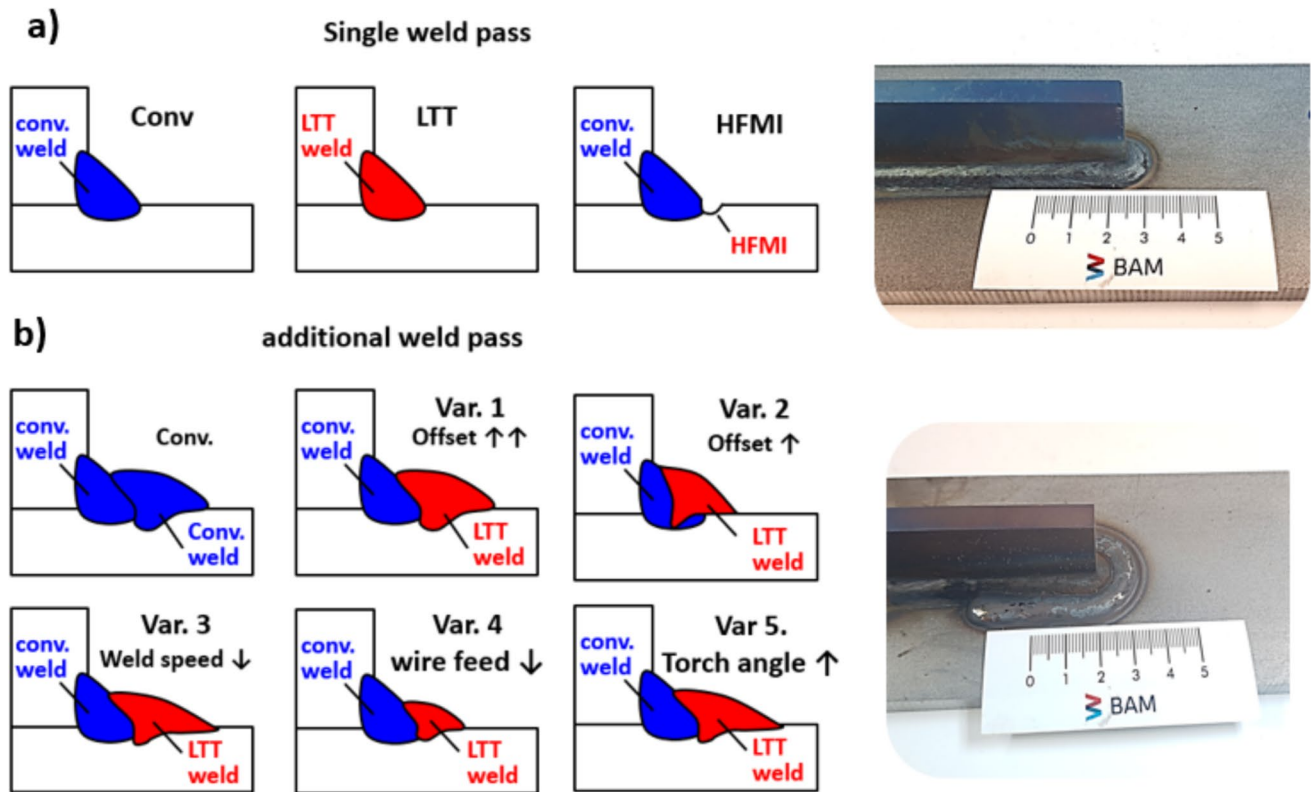


Fig. 2 Test matrix of the nine sample series with the schematic cross-sections and an example of **a** single pass and **b** additional weld pass at the front layers

Table 4 Welding parameters for the additional weld pass

| Variant Nr | 1 | 2 | 3 | 4 | 5 |
|----------------------|-------------|-------------|----------------------|----------------|---------------|
| Label | Offset ↑↑ | Offset ↑ | Rot. welding speed ↓ | Wire feed ↓ | Torch angle ↑ |
| Used Filler | LTT + conv | LTT | LTT | LTT | LTT |
| Current | 285 A | 285 A | 285 A | 180 A | 285 A |
| Voltage | 28.5 V | 28.5 V | 28.5 V | 25 V | 28.5 V |
| Welding speed | 40 cm/min | 40 cm/min | 20 cm/min | 40 cm/min | 25 cm/min |
| Offset to first pass | 4 mm | 1 mm | 4 mm | 4 mm | 5 mm |
| Wire feed | 9 m/min | 9 m/min | 9 m/min | 6 m/min | 9 m/min |
| Torch angle | 45° | 45° | 45° | 45° | 60° |

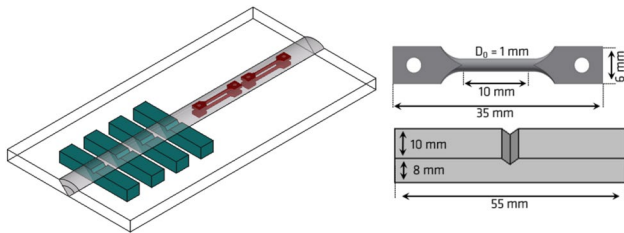
the base material. The important parameters are listed in Table 5. Round tensile and Charpy V-notch impact tests were carried out in conformity with DIN EN ISO 6892-1 [30] and DIN EN ISO 148-1:2017 [31], respectively. Since the impact test specimens were only 8 mm wide instead of the normally used 10 mm, a correction factor according to Wallin [32] was applied, the ratio of sample ligaments $A_{10 \times 10} / A_{B \times 10}$. This results in a correction factor of $100/80 = 1.25$.

Furthermore, dilatometer tests were carried out to determine the M_S and final expansion strain (FES) in the

weld metal. For this purpose, a fillet weld was welded using conventional weld metal. Subsequently, an LTT and a conventional second weld bead were applied with a welding speed of 40 cm/min. The dilatometer samples were taken from this second weld layer by electrical discharge machining (EDM) and had a length of 10 mm and a diameter of 4 mm. In addition, a dilatometer sample was taken from the base material. A previous study had shown that the welding speed had only a negligible influence on the chemical composition in the weld and thus on the M_S [15].

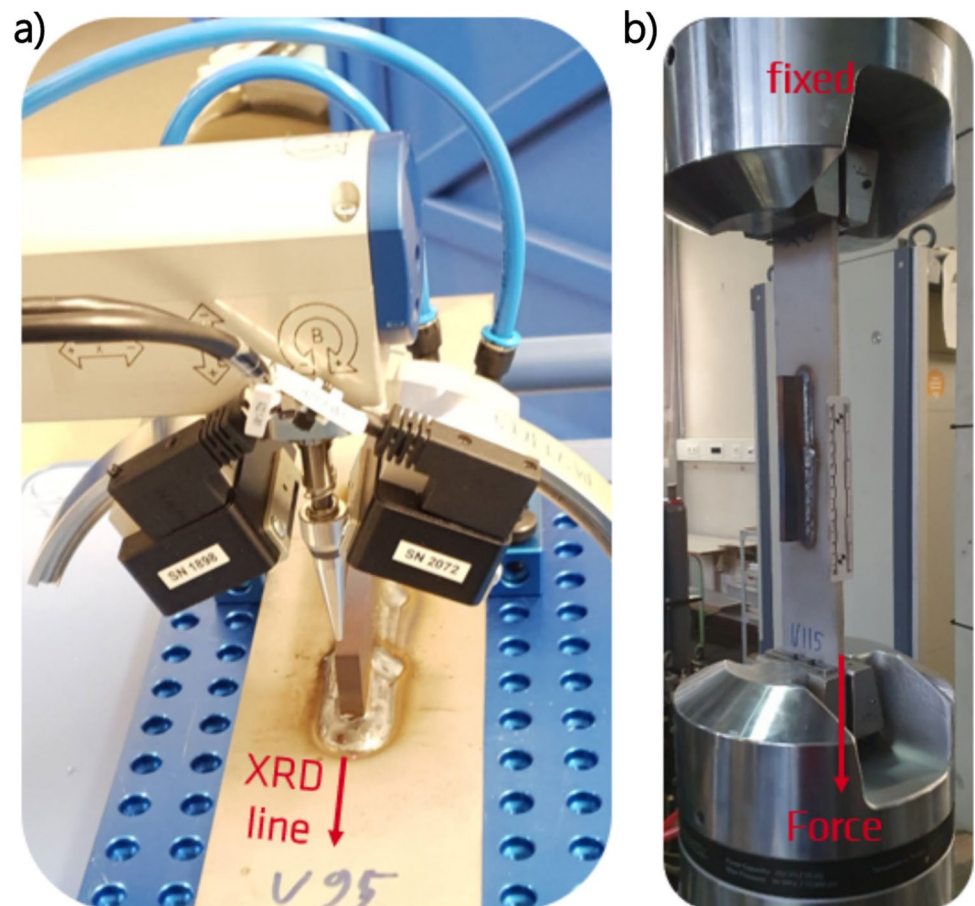
Table 5 Welding parameters for the V-butt weld

| | Wire feed | Voltage | Current | Welding speed | Arc energy |
|-------------|-----------|---------|-----------|---------------|-----------------|
| First pass | 7 m/min | 24–26 V | 196–200 A | 40 cm/min | 0.7–0.79 kJ/mm |
| Second pass | 8 m/min | 28–29 V | 220–230 A | 45 cm/min | 0.82–0.89 kJ/mm |

**Fig. 3** Schematic sketch of a two-pass V weld with extraction locations of the macro-tensile and notch-impact samples and dimensions of the tested samples

2.4 Residual stress

The residual stresses at the surface were measured using X-ray diffraction (XRD). The measurement was carried out in the HAZ of the base material at the face end. The measurement direction was transverse to the weld seam and thus

Fig. 4 **a** XRD setup for residual stress determination in the HAZ transverse to the weld and **b** fatigue testing setup with a servo hydraulic machine

in the load direction of the fatigue test. The set up is given in Fig. 4a. From the weld toe beginning, the measurement was in the HAZ 9 mm long with 11 measurement points. The residual stresses were calculated applying the $\sin^2\psi$ method [33] with a Cr-K α radiation for the 211 α diffraction line. The ψ -angles varied between 0° and 45° with 10 ψ steps. The aperture (collimator) diameter was 2 mm and the measurement time 3 s. An E -module of 215 GPa with a Poisson's ratio of 0.24 was used.

2.5 Fatigue testing

The longitudinal stiffeners were fatigue tested on a servo-hydraulic 250 kN test machine, as shown in Fig. 4b. A constant force-controlled amplitude was applied in the longitudinal direction of the stiffener. A frequency of 20 Hz and a stress ratio $\sigma_{\min}/\sigma_{\max}$ R of 0.1 were used. All tests were performed until fracture or were stopped at 5 million

Table 6 Mechanical properties of diluted weld metal and base material

| Material | σ_Y (MPa) | σ_{US} (MPa) | A_G (%) | Measured impact energy at 20 °C (J) | Corrected impact energy at 20 °C (J) |
|---------------|------------------|---------------------|-----------|-------------------------------------|--------------------------------------|
| Base material | 775 ± 20 | 828 ± 25 | 7.2 ± 0.3 | 151 ± 5 | 189 ± 5 |
| Conv. filler | 643 ± 52 | 860 ± 30 | 6.6 ± 1.3 | 26 ± 7 | 33 ± 9 |
| LTT filler | 923 ± 14 | 1155 ± 14 | 2.3 ± 0.1 | 14 ± 2 | 17 ± 2 |

cycles (run-outs). S–N curves and slope were calculated with regression analysis. The number of cycles was plotted against the stress range ($\Delta\sigma$), and the mean fatigue strength (50% survival probability) was calculated at two million cycles. The analysis does not take into account failures that occurred at the same stress range, such as a run-out [34].

3 Results and discussion

3.1 Materials characterization and dilatometer tests

The results of the materials characterization are summarized in Table 6, which lists the yield strength σ_Y , ultimate tensile

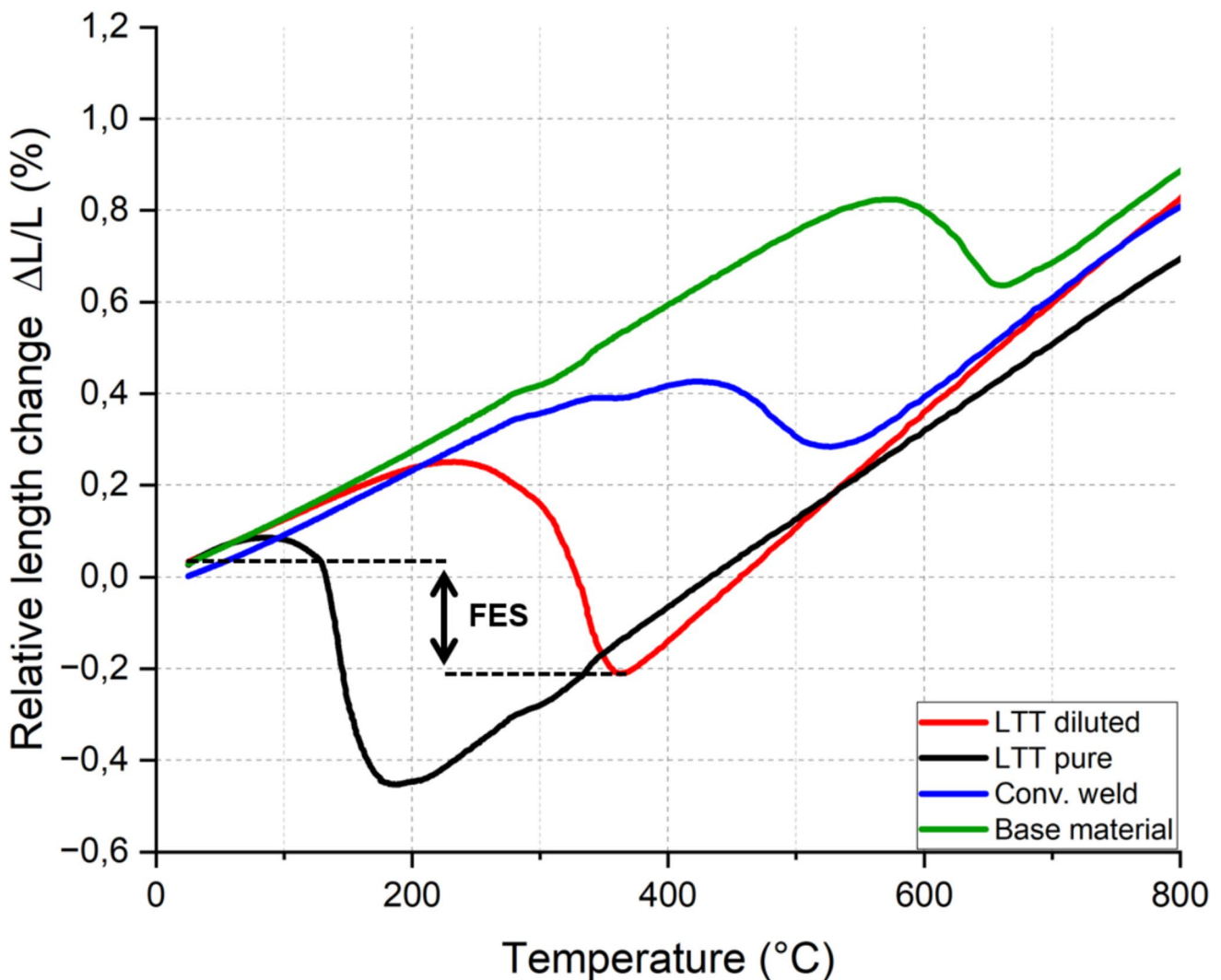


Fig. 5 Dilatometer cooling curves with a cooling time of $t_{8/5}$ of 5 s. The FES is plotted exemplarily for the diluted LTT.

Table 7 Transformation temperatures and final expansion strain from the dilatometer test

| Dilatometer sample | Transformation start temperature (°C) | Transformation finish temperature (°C) | FES (%) |
|--------------------|---------------------------------------|--|---------|
| LTT diluted | 364 | 233 | 0.24 |
| LTT pure | 217 | 106 | 0.48 |
| Conv. weld | 520 | 412 | -0.28 |
| Base Material | 650 | 550 | -0.64 |

strength σ_{US} , uniform elongation A_G (%) and the measured and corrected impact energy. The tensile test values of the base material and diluted conventional weld metal correspond to the specific data sheets. The values of the diluted LTT weld metal are significantly higher in terms of yield strength and tensile strength but lower in elongation and are

therefore similar to those found in the study by Hensel et al. [22] ($\sigma_Y = 944$ MPa, $\sigma_{US} = 1121$ MPa and $A_G = 3.4\%$). The corrected toughness values of the diluted LTT weld metal are at 17 J, approximately 50% lower than those of the conventional weld metal. The values reported by Hensel et al. [22] are at 22 J, in a similar range for the same shielding gas M21. The analysis indicates that the diluted LTT weld metal exhibits only minor changes in the mechanical properties of the pure LTT weld metal reported in the study by Hensel et al. [22]. Therefore, the high yield and tensile strength, as well as the low toughness, are similar to those of the undiluted LTT weld metal.

The results of the dilatometer test are summarized in Fig. 5 and Table 7. The pure LTT and the diluted LTT weld metal have a lowered M_S and a positive FES. In contrast, the conventional weld metal and the base material have higher M_S temperatures of 520 °C and 650 °C, respectively. In the

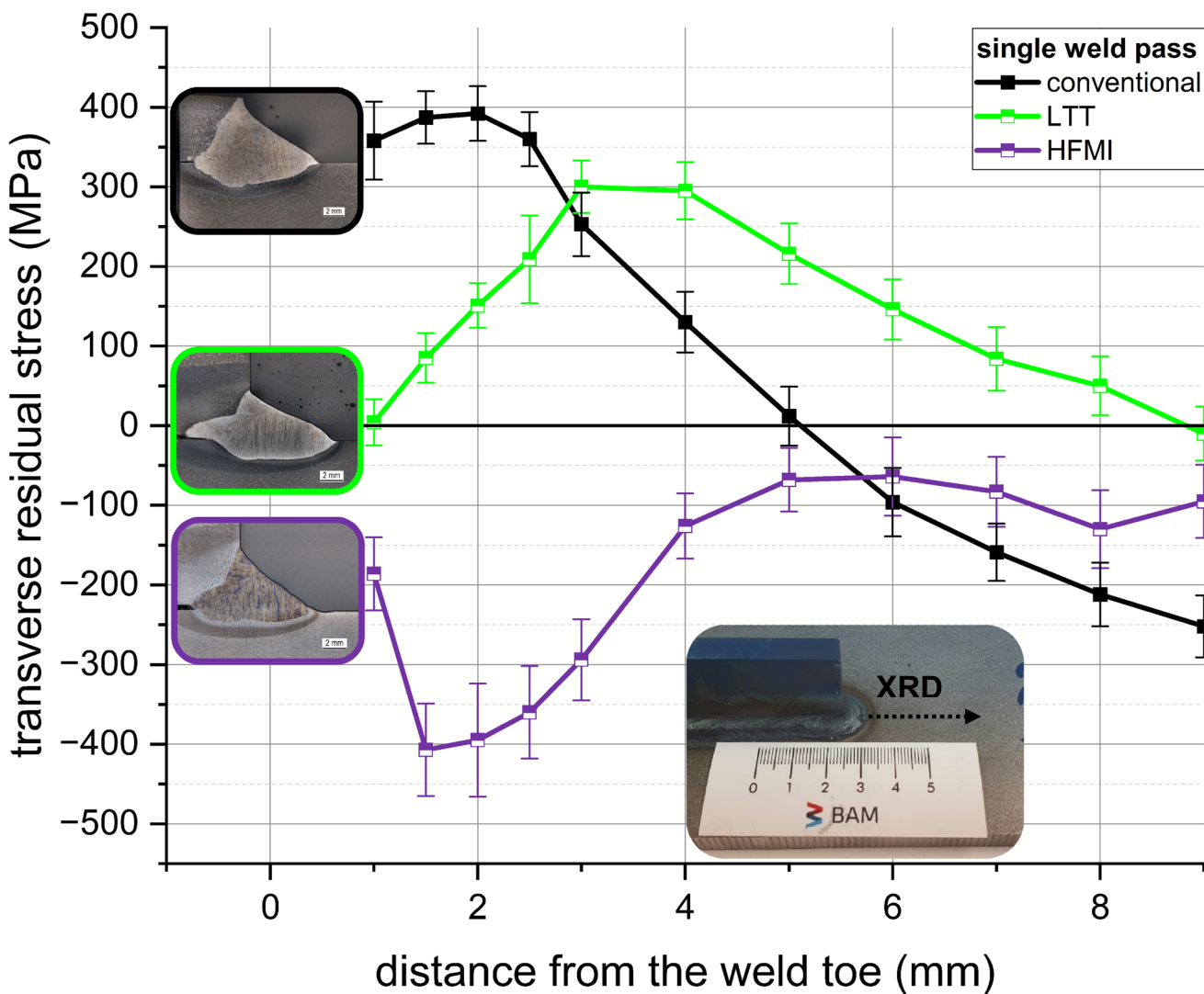


Fig. 6 Residual stress in the HAZ for single weld pass

Fig. 7 Residual stress in the HAZ for an additional weld pass

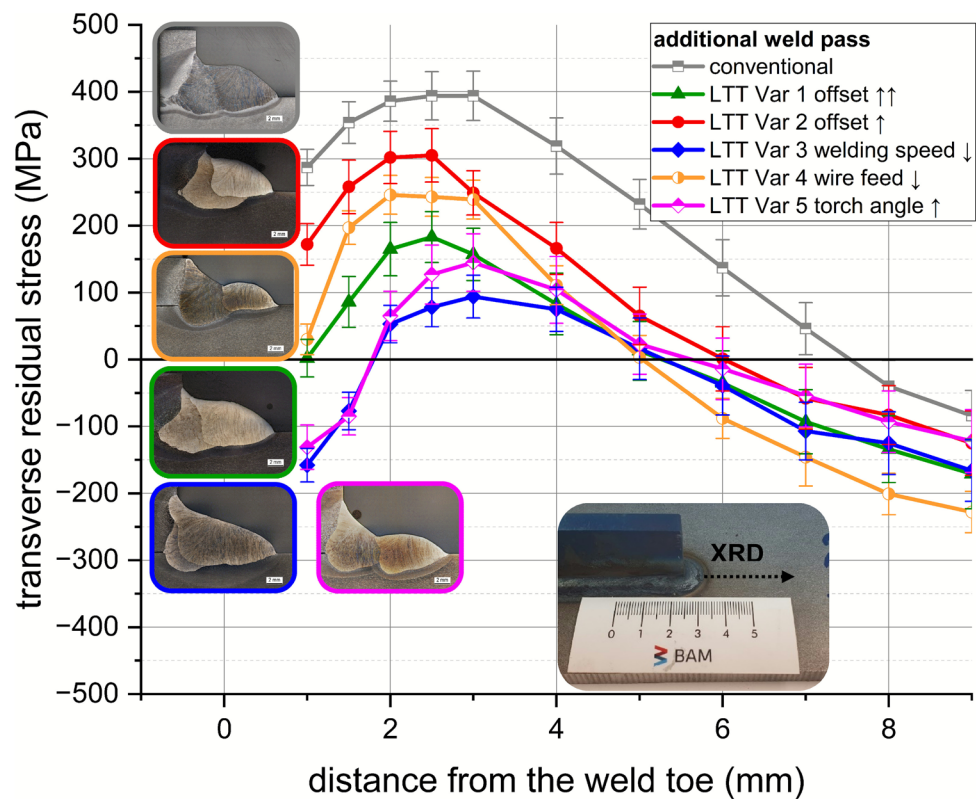


Table 8 Residual stress at weld toe and maximum residual stress in the HAZ for all variants

| Sample description | Transverse residual stress at weld toe (MPa) | Maximum residual stress in HAZ (MPa) |
|--|--|--------------------------------------|
| Single weld pass | | |
| Conventional | 358 | 392 |
| LTT | 4 | 300 |
| HFMI | -186 | -64 |
| Additional weld pass | | |
| Conventional offset $\uparrow\uparrow$ | 287 | 394 |
| LTT var 1 offset $\uparrow\uparrow$ | 2 | 183 |
| LTT var 2 offset \uparrow | 172 | 305 |
| LTT var 3 welding speed \downarrow | -158 | 94 |
| LTT var 4 wire feed \downarrow | 30 | 246 |
| LTT var 5 torch angle \uparrow | -131 | 145 |

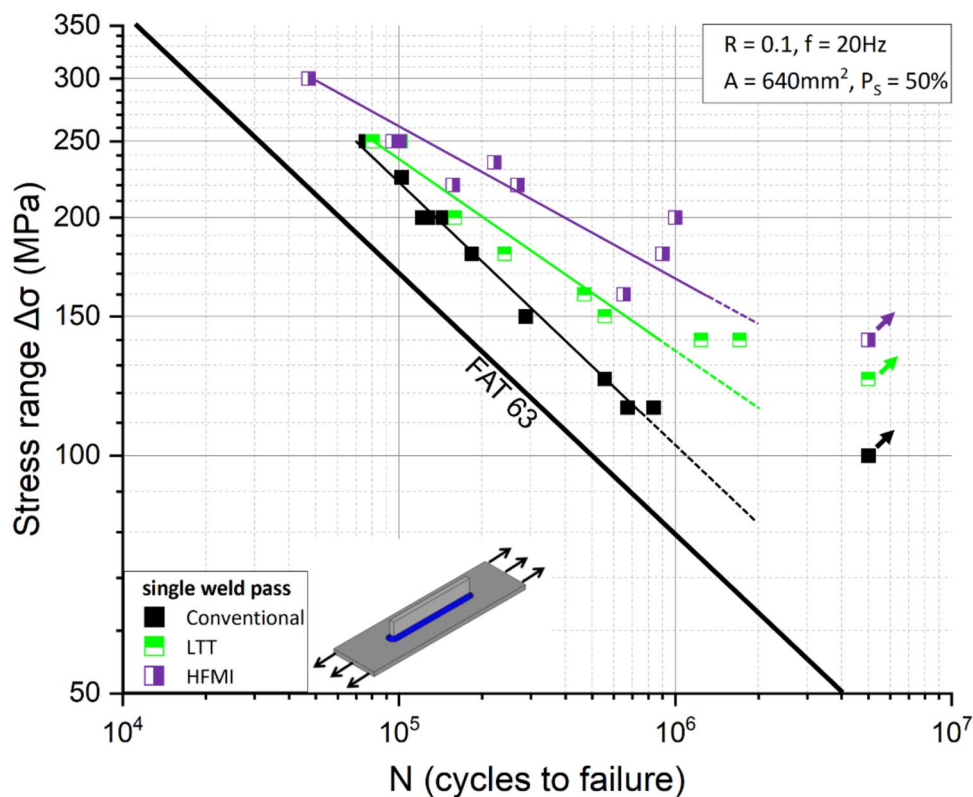
case of the base material, it is necessary to assume a bainitic transformation rather than martensite formation. The higher transformation temperatures lead to a negative FES for the base material and the conventional weld filler. Thus, a residual stress-reducing LTT effect can be expected for the LTT weld filler in the pure and diluted states, whereas this is not the case for the conventional weld filler or the base material.

3.2 Residual stress

The determined residual stresses in the HAZ are illustrated in Fig. 6 for single weld pass and in Fig. 7 for stiffeners with an additional weld pass. The residual stresses are presented as a function of the distance from the weld toe, with 0 mm being the position of the weld toe. For clarity, the values at the weld toe and the maximum residual stress in the HAZ are listed in Table 8. The single pass with conventional filler metal exhibits the highest residual stresses at the weld toe and in the maximum of the HAZ. The use of the LTT filler as a single pass reduces the residual stress. The LTT filler causes a reduction of approximately 350 MPa at the weld toe and 100 MPa at the maximum compared to the conventional weld. The most residual stress reduction turns out for the HFMI samples for the single pass with -186 MPa compressive residual stress at the weld toe. These values show the same trend as those in the studies by Schubnell et al. [8] (for HFMI) and Grönlund et al. [35] (for S700M conventional welded). The HFMI samples were partly determined within the radius of the HFMI treatment, which is why the residual stresses remain in the compressive zone and are much lower than all other residual stress values.

Using LTT welding consumables for the additional pass, a residual stress reduction occurs, although to varying degrees (Fig. 7). A welding speed reduction and a higher torch angle

Fig. 8 S–N curves for the single weld pass samples



achieve the strongest effect of residual stress reduction in the weld toe (≈ -150 MPa) and at the maximum (≈ 100 to 150 MPa) of the HAZ. A lower offset leads to a residual stress reduction at the weld toe of 172 MPa and a maximum of 305 MPa. A high offset and a lower wire feed speed result

in ≈ 0 MPa residual stress at the weld toe, but the peak in both curves differs considerably (170 to 250 MPa). The results of additional front face layers confirm that the LTT welding consumables reduce the tensile residual stress. Adding a second weld pass with conventional filler metal instead does not lead to a significant reduction in residual stresses at the weld toe and the maximum, which is also confirmed in the results of Harati et al.'s [17] study.



Fig. 9 Specimen with LTT single weld pass after fatigue testing. The crack propagated along the weld toe

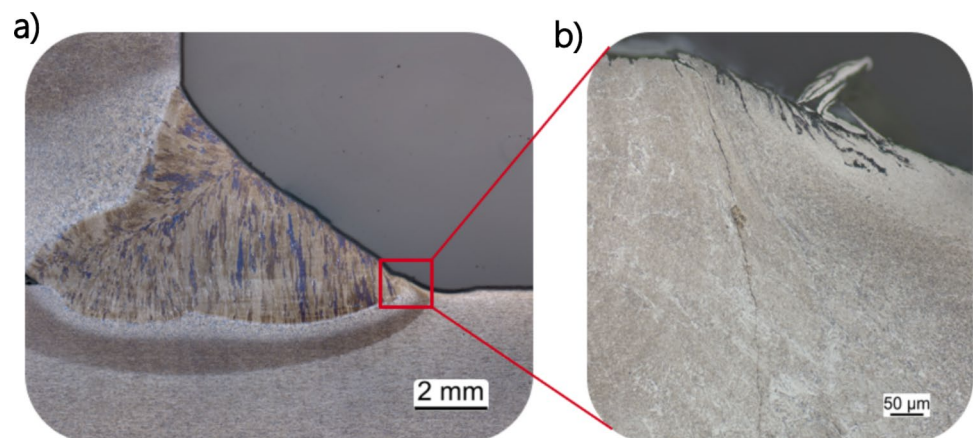
3.3 Fatigue testing

The S–N curves are plotted for the stiffeners with a single weld pass in Fig. 8 and with an additional pass in Fig. 11. For a 150 -mm-long stiffener plate, the IIW fatigue design curve FAT 63 is included as a reference [21]. All tested specimens failed at the weld toe, including the LTT single pass (Fig. 9). Table 9 summarizes the following results: fatigue strength at 2 million cycles, calculated slope m , and improvement of the mean fatigue strength, which is the ratio of the fatigue strength between the individual sample and the conventional single pass sample.

The single-pass welded longitudinal stiffeners exhibit very different S–N curves depending on the sample type. The conventional longitudinal stiffener has a slope of $m=3.0$, which coincidentally corresponds to FAT 63. The mean fatigue strength of 81 MPa is within the range of other values for the same steel grade, thickness, and stiffener

Table 9 Data of the S–N curves and the obtained fatigue strength

| Sample description | Number of samples (–) | Slope, m (–) | Mean fatigue strength $\Delta\sigma_{c,50\%}$ (MPa) | Improvement of $\Delta\sigma_{c,50\%}$ (%) |
|--|-----------------------|----------------|---|--|
| Single weld pass | | | | |
| Conventional | 11 | 3.0 | 81 | – |
| LTT | 9 | 4.5 | 121 | 49 |
| HFMI | 10 | 5.1 | 146 | 79 |
| Additional weld pass | | | | |
| Conventional offset $\uparrow\uparrow$ | 8 | 3.3 | 83 | 1 |
| LTT var 1 offset $\uparrow\uparrow$ | 11 | 5.1 | 166 | 104 |
| LTT var 2 offset \uparrow | 9 | 5.4 | 156 | 92 |
| LTT var 3 welding speed \downarrow | 9 | 7.6 | 196 | 140 |
| LTT var 4 wire feed \downarrow | 7 | 5.2 | 138 | 69 |
| LTT var 5 torch angle \uparrow | 9 | 6.6 | 194 | 138 |

Fig. 10 Micrograph of an HFMI fatigue-tested sample of the non-ruptured site: **a** full cross-section and **b** magnified section of the sample with a rough surface and crack initiation

length (e.g., Grönlund et al. [35], $\rightarrow \Delta\sigma_{c,50\%} = 80$ MPa). The LTT single weld pass increases the slope m to 4.5 and exhibits a mean fatigue strength of 121 MPa, which represents an improvement of 49% in fatigue behavior. The LTT fatigue values are within the range of statistical values from Bartsch [19]. All samples show crack initiation and propagation at the weld toe, as exemplified in Fig. 9. Despite the reduced toughness of the LTT welding consumable, no visible cracks occurred in the weld root during fatigue testing. However, as the specimen has a gap in the middle of the stiffener and is therefore not fully welded through, the possibility of crack initiation at the weld root cannot be completely excluded. The HFMI-treated samples showed the best values for the single-pass longitudinal stiffener, with a slope of 5.1 and $\Delta\sigma_{c,50\%} = 146$ MPa; the improvement is 79%. Figure 10 gives a micrograph of an HFMI sample after fatigue testing on the non-ruptured side. It is noteworthy that crack initiation occurred next to the HFMI-treated zone, where the surface is very rough, which could explain the relatively high scatter of the HFMI fatigue tests. One possible explanation is that the HFMI pin was positioned too far into the base material.

Since the HFMI process was applied manually, precise treatment of the weld toe—especially at the face ends—was difficult to achieve. Nevertheless, even the outliers of the HFMI-treated longitudinal stiffeners show significantly higher fatigue strength than untreated samples.

All in all, for the single-weld-pass stiffeners, HFMI performed best, LTT was in the middle range, and conv. performed worst. These gradations of improvements in fatigue strength are consistent with Lixing et al.'s [16] results, in which longitudinal stiffeners with base-material yield strengths of 253 MPa were investigated.

The S–N curves with additional weld pass at the front faces are given in Fig. 11. The additional weld pass with a conventional filler shows a slope of $m = 3.3$ and $\Delta\sigma_{c,50\%} = 83$ MPa and performs similarly to the conventional single pass samples. All samples with an additional LTT pass show a significant improvement in fatigue strength. LTT Variant 4 (wire feed \downarrow) shows with $m = 5.2$ and a $\Delta\sigma_{c,50\%} = 138$ MPa an almost similar increase as HFMI treated single pass samples with an improvement of 67%. Variants 2 (offset \uparrow) and 1 (offset $\uparrow\uparrow$) give a

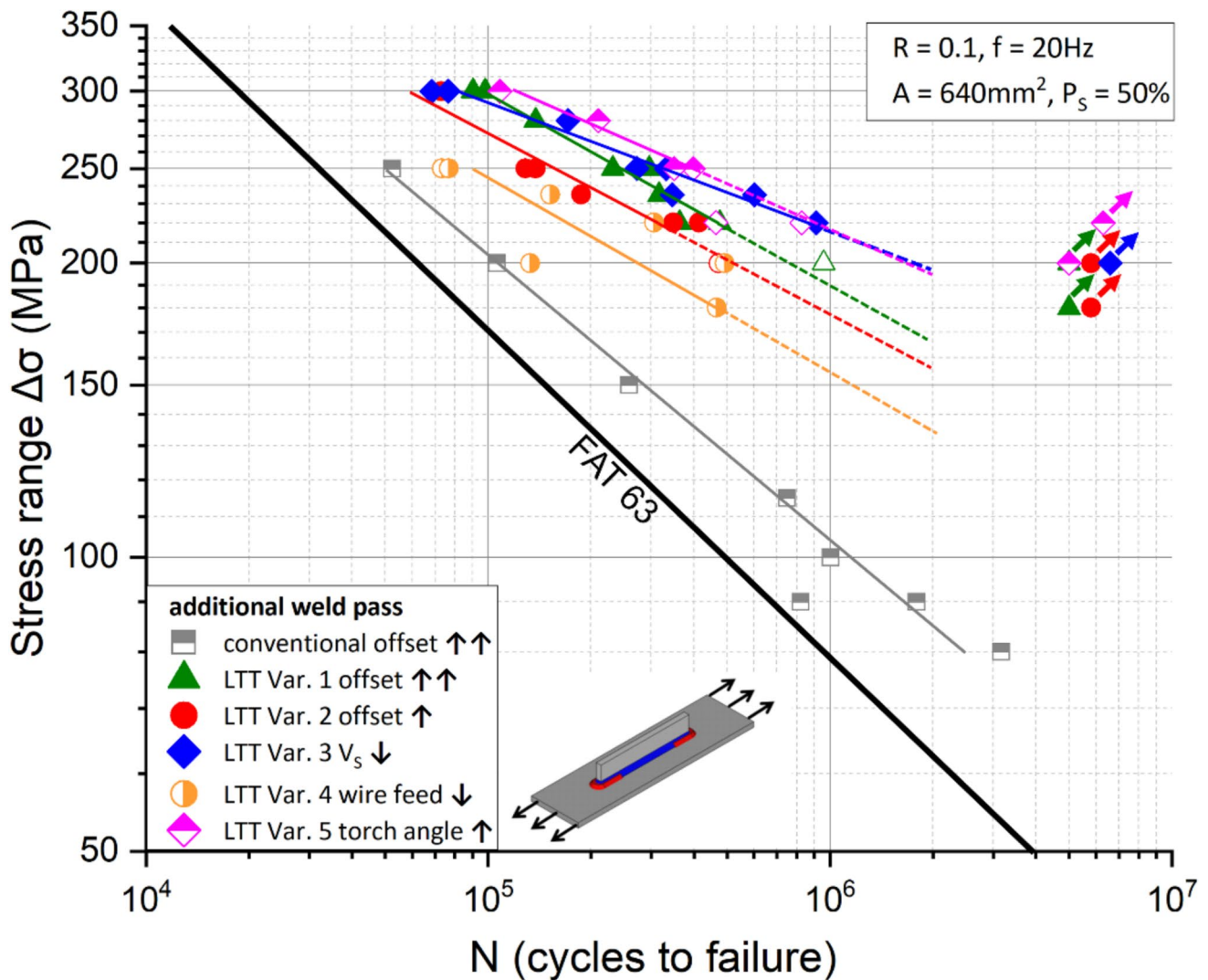


Fig. 11 S–N curves for the additional weld pass samples

higher improvement in fatigue strength with 156.0 MPa and 166.3 MPa, respectively. Variants 3 (welding speed ↓) and 5 (torch angle ↑) have the best fatigue results with a slope of $m = 7.6$ and $m = 6.5$; the mean fatigue strength is at $\Delta\sigma_{c,50\%} = 196$ MPa and $\Delta\sigma_{c,50\%} = 194$ MPa. This is an improvement of 137% and 135% for variants 3 and 5, respectively.

Generally, specimens characterized by low tensile residual stresses in the fatigue critical HAZ show an increase in the slope m . At lower stress ranges, compressive or low tensile residual stresses delay fatigue crack initiation more than they do in higher stress ranges. This can explain the higher S–N slopes observed for specimens with low residual stresses and the resulting increase in mean fatigue strength. This flatness of the S–N curves is observed in the literature

both in LTT samples from the work of Harati et al. [17] and in HFMI samples from the work of Schubnell et al. [28].

The results demonstrate that the use of LTT welding filler has a positive effect on fatigue strength in single and additional pass welded longitudinal stiffeners. However, there is a clear difference between the two kinds. The single LTT layer does not achieve the same increase in fatigue strength as the HFMI-treated samples. In the case of the LTT as an additional pass, the specimens significantly exceeded the HFMI results in four of five cases. The choice of welding parameters and the resulting geometry are important factors in this context. In variant 4, a lower wire feed speed added the smallest total amount of LTT weld filler in the fatigue-critical zone, so the LTT effect is weaker. Although for variant 4 the residual stress at the weld toe was similar

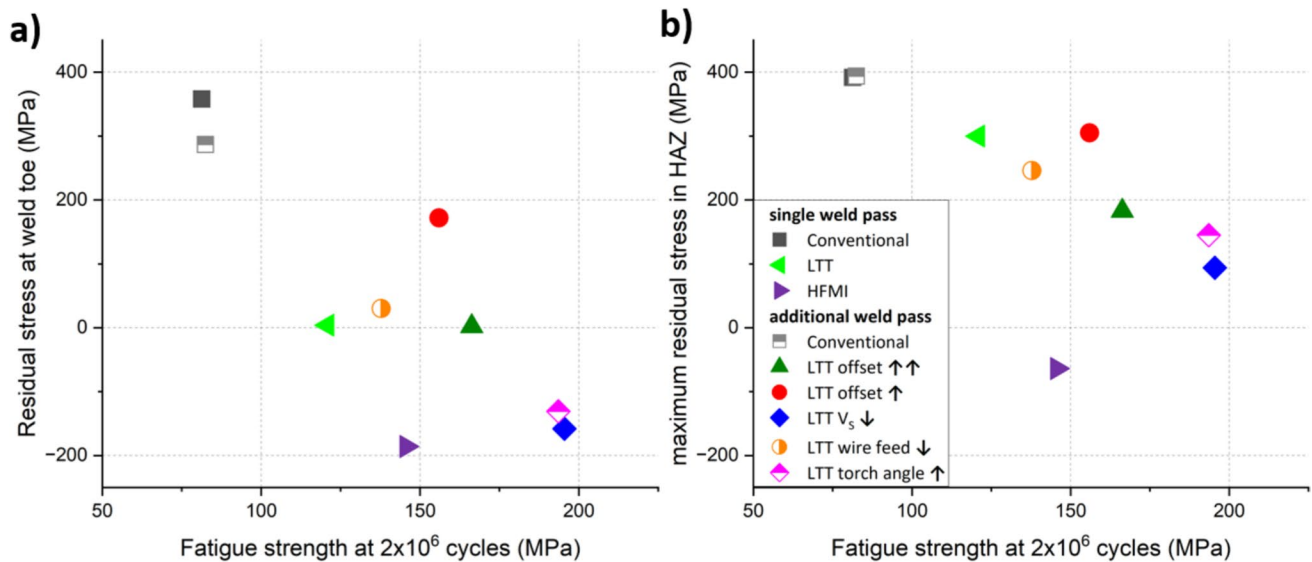


Fig. 12 Correlation between the mean fatigue strength and **a** the residual stress at the weld toe and **b** the maximum residual stress in the HAZ

to that in variant 1 and lower than in variant 2, the fatigue results were better in variants 1 and 2. The first two variants exhibit a higher amount of added LTT weld filler. The LTT effect is most pronounced in variants 3 and 5, as these have the slowest welding speed and therefore the highest amount of LTT was applied. This is one more indication that the amount of LTT filler used is crucial for fatigue behavior. The fact that the additional weld pass with LTT filler in most cases achieves better results in fatigue strength, higher slope than a single LTT pass, and performs much better than the conventional welding fillers is in accordance with the works of Harati et al. [17] and Shiga et al. [24]. In both studies, an LTT filler was applied as an additional pass in the fatigue-critical zone and achieved an increase in fatigue strength.

3.4 Correlation between residual stresses and fatigue strength

A qualitative correlation can be identified between the residual stresses determined by XRD measurements and the corresponding fatigue strength values. As an example, LTT variants 3 and 5 exhibit the lowest residual stresses both at the weld toe and at the maximum in the HAZ, while simultaneously achieving the highest fatigue strength. In contrast, conventional welds (both the single-pass and the additional pass) show the highest residual stresses and the lowest fatigue strength. A comparison between LTT variant 2 (Offset ↑) and variant 4 (Wire feed ↓) reveals that variant 2 demonstrates superior fatigue performance—approximately 30 MPa higher in $\Delta\sigma_{c,50\%}$ —despite higher residual stresses at the weld toe. Nonetheless, both variants show significantly

improved fatigue strengths compared to conventional welds, even though the difference in residual stress between variant 2 and the conventional specimens is only about 100 MPa.

Figure 12 presents the fatigue strength at 2 million cycles on the x-axis against (a) the residual stress at the weld toe and (b) the maximum residual stress in the HAZ on the y-axis. In both cases, an inverse relationship is observed: lower residual stresses correspond to higher fatigue strengths. Although this trend exhibits some scatter in the weld toe data, it becomes more distinct—displaying an approximately linear relationship—when considering the maximum residual stress within the HAZ.

Only the HFMI values differ greatly between the two curves. They have the highest residual compressive stresses; however, they do not have the best fatigue values. One possible explanation is that factors such as the radius at the weld toe and the hardening in the HAZ also play a role in HFMI. Furthermore, as shown in Fig. 10, the rough surface adjacent to the HFMI-treated zone serves as the crack initiation site.

Figure 12 shows that the residual stress reduction due to the LTT effect has a positive effect on the fatigue strength; however, the improvement depends on the weld shape. Using LTT welding fillers leads to a residual stress reduction in the fatigue-critical area the farther the weld toe is from the stiffener sheet, as shown in a previous study [15]. This trend continues for the fatigue strength. In this case as well, LTT series show similar dilution, since only one type of LTT welding filler was used; nevertheless, the fatigue behavior varies. This demonstrates that knowing the residual stress in the HAZ is important for estimating the fatigue strength of longitudinal stiffeners when using the LTT effect.

4 Conclusion

In this study, longitudinal stiffeners welded with an LTT filler were tested for residual stresses and fatigue strength. In nine sample series, the weld design was realized both as a single weld pass and—with varying welding parameters—and as an additional pass in the fatigue-critical areas. In addition, the mechanical properties of the LTT filler in its diluted state were investigated. The following can be stated:

1. The mechanical properties of the diluted LTT weld metal exhibit reduced toughness but higher yield and tensile strength compared with the conventional filler.
2. The reduced M_S of the LTT filler resulted in reduced residual stresses compared to the conventional filler.
3. No undesired root crack propagation was observed during the fatigue tests in this study, not even for a single weld pass with LTT.
4. The single-pass LTT samples perform better than single and additional-pass conventional samples. HFMI treatment had the greatest effect on increasing fatigue strength for single-pass samples. The LTT as an additional weld achieved the best fatigue results.
5. The residual stress reduction, which varies depending on the weld shape, is crucial for the fatigue strength. The lower the maximum residual stresses in the HAZ, the better the fatigue strength in the case of LTT welded specimens.
6. When LTT fillers are used, the increase in fatigue strength depends not only on the chemical composition and the resulting M_S but also on the weld shape and the associated residual stress state.

Acknowledgements The research project IGF 22560 N/DVS 09.3540 “Hybrid use of LTT welding consumables to improve the fatigue strength of high-strength steel components” by the Research Association on Welding and Allied Processes of the DVS, Düsseldorf, was supported by the Federal Ministry for Economic Affairs and Climate Action through the German Federation of Industrial Research Associations (AiF) as part of the program for promoting industrial cooperative research (IGF) on the basis of a decision of the German Bundestag. The project was carried out at the Bundesanstalt für Materialforschung und -prüfung (BAM) and the Fraunhofer Institute for Mechanics of Materials (IWM).

Author contribution Conceptualization: Martin Huebner, Florian Dittmann, Arne Kromm, Igor Varfolomeev, and Thomas Kannengiesser; methodology: Martin Huebner; experiments: Martin Huebner and Florian Dittmann; evaluation: Martin Huebner and Florian Dittmann; writing—review and editing: Martin Huebner and Arne Kromm; funding acquisition: Arne Kromm, Igor Varfolomeev, and Thomas Kannengiesser; supervision: Arne Kromm and Thomas Kannengiesser.

Funding Open Access funding enabled and organized by Projekt DEAL.

Data availability Not applicable

Declarations

Competing interests The authors declare no competing interests.

Open Access This article is licensed under a Creative Commons Attribution 4.0 International License, which permits use, sharing, adaptation, distribution and reproduction in any medium or format, as long as you give appropriate credit to the original author(s) and the source, provide a link to the Creative Commons licence, and indicate if changes were made. The images or other third party material in this article are included in the article’s Creative Commons licence, unless indicated otherwise in a credit line to the material. If material is not included in the article’s Creative Commons licence and your intended use is not permitted by statutory regulation or exceeds the permitted use, you will need to obtain permission directly from the copyright holder. To view a copy of this licence, visit <http://creativecommons.org/licenses/by/4.0/>.

References

1. Marquis G (2010) Failure modes and fatigue strength of improved HSS welds. *Eng Fract Mech* 77:2051–2062. <https://doi.org/10.1016/j.engfracmech.2010.03.034>
2. Nitschke-Pagel T, Wohlfahrt H (2002) Residual stresses in welded joints - sources and consequences. *Ecrs 6: proceedings of the 6th European conference on residual stresses* 404–7:215–224. <https://doi.org/10.4028/www.scientific.net/MSF.404-407.215>
3. Yildirim HC, Leitner M, Marquis GB, Stoschka M, Barsoum Z (2016) Application studies for fatigue strength improvement of welded structures by high-frequency mechanical impact (HFMI) treatment. *Eng Struct* 106:422–435. <https://doi.org/10.1016/j.engstruct.2015.10.044>
4. Cui C, Zhang QH, Bao Y, Bu YZ, Luo Y (2019) Fatigue life evaluation of welded joints in steel bridge considering residual stress. *J Constr Steel Res* 153:509–518. <https://doi.org/10.1016/j.jcsr.2018.11.003>
5. Gericke A, von Borstel T, Strandberg M, Henkel KM (2025) Fatigue strength of blast cleaned and stress relief annealed butt joints made of structural steel S355J2+N for offshore wind support structures. *Int J Fatigue*. <https://doi.org/10.1016/j.ijfatigue.2024.108711>
6. Kirkhope KJ, Bell R, Caron L, Basu RI, Mas K-T (1999) Weld detail fatigue life improvement techniques. Part 1: review 12:447–474. [https://doi.org/10.1016/S0951-8339\(99\)00013-1](https://doi.org/10.1016/S0951-8339(99)00013-1)
7. Marquis GB, Yildirim HC (2015) Fatigue improvement of welded steel joints by high frequency mechanical impact treatment. *Materialwiss Werkst* 46:136–144. <https://doi.org/10.1002/mawe.20140368>
8. Schubnell J, Pontner P, Wimpory RC, Farajian M, Schulze V (2020) The influence of work hardening and residual stresses on the fatigue behavior of high frequency mechanical impact treated surface layers. *Int J Fatigue*. <https://doi.org/10.1016/j.ijfatigue.2019.105450>
9. Ooi SW, Garnham JE, Ramjaun TI (2014) Review: low transformation temperature weld filler for tensile residual stress reduction. *Mater Des* 56:773–781. <https://doi.org/10.1016/j.matdes.2013.11.050>
10. Kromm A, Dixneit J, Kannengiesser T (2014) Residual stress engineering by low transformation temperature alloys—state of the art and recent developments. *Welding World* 58:729–741. <https://doi.org/10.1007/s40194-014-0155-6>

11. Ohta A, Matsuoka K, Nguyen NT, Maeda Y, Suzuki N (2003) Fatigue strength improvement of lap joints of thin steel plate using low-transformation-temperature welding wire. *Weld J* 82:78s-83s. <Go to ISI>://WOS:000186768400016
12. Akyel F, Gamerding M, Olschok S, Reisgen U, Schwedt A et al (2022) Residual stress reduction with the LTT effect in low carbon manganese-steel through chemical composition manipulation using dissimilar filler material in laser beam welding. *Metals*. <https://doi.org/10.3390/met12060911>
13. Hosseini SA, Gheisari K, Moshayedi H, Ahmadi MR, Warchomiccka F et al (2021) Assessment of the chemical composition of LTT fillers on residual stresses, microstructure, and mechanical properties of 410 AISI welded joints. *Weld World* 65:807–823. <https://doi.org/10.1007/s40194-020-01064-1>
14. Wu SP, Wang DP, Zhang Z, Li CN, Liu XG et al (2019) Mechanical properties of low-transformation-temperature weld metals after low-temperature postweld heat treatment. *Sci Technol Weld Join* 24:112–120. <https://doi.org/10.1080/13621718.2018.1492776>
15. Hübner M, Dittmann F, Kromm A, Varfolomeev I, Kannengiesser T (2025) Residual stress reduction using a low transformation temperature welding consumable with focus on the weld geometry. *Weld World*. <https://doi.org/10.1007/s40194-025-02094-3>
16. Lixing WDH, Wenxian W, Yufeng Z (2013) Ultrasonic peening and low transformation temperature electrodes used for improving the fatigue strength of welded joints. *Weld World*. <https://doi.org/10.1007/BF03266425>
17. Harati E, Karlsson L, Svensson LE, Dalaei K (2015) The relative effects of residual stresses and weld toe geometry on fatigue life of weldments. *Int J Fatigue* 77:160–165. <https://doi.org/10.1016/j.ijfatigue.2015.03.023>
18. Igwemezie V, Mehmanparast A, Ganguly S (2024) Assessment of fatigue crack growth resistance of newly developed LTT alloy composition for the repair of high strength steel structures. *J Adv Join Process*. <https://doi.org/10.1016/j.jajp.2024.100226>
19. Bartsch H (2025) Data-driven investigations on the fatigue resistance of joints welded with low-transformation-temperature effects. *J Constr Steel Res*. <https://doi.org/10.1016/j.jcsr.2025.109762>
20. (2010) DIN EN 1993–1–9 :2005+AC:2009, Eurocode 3: Bemessung und Konstruktion von Stahlbauten – Teil 1–9: Ermüdung
21. Hobbacher AF (2009) The new IIW recommendations for fatigue assessment of welded joints and components - a comprehensive code recently updated. *Int J Fatigue* 31:50–58. <https://doi.org/10.1016/j.ijfatigue.2008.04.002>
22. Hensel J, Kromm A, Nitschke-Pagel T, Dixneit J, Dilger K (2020) Capability of martensitic low transformation temperature welding consumables for increasing the fatigue strength of high strength steel joints. *Mater Test* 62:891–899. <https://doi.org/10.3139/120.111562>
23. Francis JA, Stone HJ, Kundu S, Bhadeshia HKDH, Rogge RB et al (2009) The effects of filler metal transformation temperature on residual stresses in a high strength steel weld. *J Press Vessel Technol*. <https://doi.org/10.1115/1.3122036>
24. Shiga C, Murakawa H, Hiraoka K, Osawa N, Yajima H et al (2017) Elongated bead weld method for improvement of fatigue properties in welded joints of ship hull structures using low transformation temperature welding materials. *Weld World* 61:769–788. <https://doi.org/10.1007/s40194-017-0439-8>
25. (2012) DIN EN ISO 16834 Welding consumables – wire electrodes, wires, rods and deposits for gas shielded arc welding of high strength steels (German Version)
26. Steven W, Haynes AG (1956) The temperature of formation of martensite and bainite in low-alloy steels. *J Iron Steel Inst* 183:349–359
27. Wu SP, Wang DP, Zhang Z, Li CN, Liu XG et al (2019) Effect of dilution on fatigue behaviour of welded joints produced by low-transformation-temperature fillers. *Sci Technol Weld Join* 24:601–608. <https://doi.org/10.1080/13621718.2019.1576272>
28. Schubnell J, Hanji T, Tateishi K, Gkatzogiannis S, Ummerhofer T et al (2025) Quantifying the intensity of high-frequency mechanical impact treatment. *Weld World* 69:125–137. <https://doi.org/10.1007/s40194-024-01812-7>
29. Gary B, Marquis ZB (2016) IIW recommendations for the HFMI treatment, for improving the fatigue strength of welded joints. IIW Collection. <https://doi.org/10.1007/978-981-10-2504-4>
30. DIN EN ISO 6892–1 (2020) Metallic materials - tensile testing - Part 1: Method of test at room temperature (ISO 6892–1:2019), German version
31. DIN EN ISO 148–1 (2017) Metallic materials - Charpy pendulum impact test - Part 1: Test method (ISO 148-1:2016); German version EN ISO 148–1:2016
32. Wallin K (2011) Fracture toughness of engineering materials: estimation and application. EMAS Publishing, Warrington, UK
33. Macherauch E, Müller P (1961) Das $\sin^2\psi$ -Verfahren der röntgenographischen Spannungsmessung. *Z Angew Phys* 13(7):305–312
34. DIN 50100 (2022) Schwingfestigkeitsversuch - Durchführung und Auswertung von zyklischen Versuchen mit konstanter Lastamplitude für metallische Werkstoffproben und Bauteile, Berlin, 2016
35. Grönlund K, Ahola A, Riski J, Pesonen T, Lipiäinen K et al (2024) Overload and variable amplitude load effects on the fatigue strength of welded joints. *Weld World* 68:411–425. <https://doi.org/10.1007/s40194-023-01642-z>

Publisher's Note Springer Nature remains neutral with regard to jurisdictional claims in published maps and institutional affiliations.